

THE TIME-DEPENDENT ELECTRON DENSITY AND MAGNETIC FIELD DISTRIBUTIONS IN A 70-ns PLASMA OPENING SWITCH

A. Weingarten, C. Grabowski, A. Fruchtman, and Y. Maron

Faculty of Physics, Weizmann Institute of Science, Rehovot 76100, Israel

ABSTRACT

The time-dependent two-dimensional electron density distribution is determined for the first time during the operation of a short-conduction plasma opening switch. The electron density, resolved in 3-D, is determined from the line intensities of different ions doped into the plasma. A rise in the electron density followed by a drop is observed to propagate from the generator towards the load at the proton Alfvén velocity. Based on spectroscopic magnetic field and ion velocity measurements, the density evolution can be explained as pushing of the protons ahead of the propagating magnetic piston, followed by magnetic field penetration into the rest of the plasma composed of the lower-density heavier ions.

I. Introduction

Plasma Opening Switches (POS's) are used for voltage and power multiplication and in inductive energy storage systems that conduct currents during periods ranging from 50 ns to over 1 μ s[1] before opening into a load. Scaling laws[2] for the POS's were shown to have good agreement with long-conduction POS experiments. The plasma dynamics in such POS's have been investigated using laser interferometry[2], and the magnetic field was studied using B-dot loops[1] and laser induced fluorescence[3]. Studies of short-duration (≤ 100 ns) POS's[1] were more limited, consisting of current and voltage measurements, studying the prefilled plasma parameters, and energetic particles emitted from the plasma. Magnetic field evolution was measured by B loops[1]. In a previous publication[4] we have described the measurements of the two-dimensional magnetic field penetration into a positive-polarity POS plasma. The field penetration was quantitatively explained by an EMHD (Hall) model[5], which used as an input the prefilled plasma density distribution and assumed that n_e does not change appreciably during the current pulse, an assumption supported by previous results [6].

II. Experimental System

Figure 1 shows the POS setup. The diameters of the cathode and anode are 4 and 9 cm, respectively, and the plasma axial length is 10 cm giving upstream and downstream inductances of 95 and 25 nH, respectively. A 170 kA, 85 ns quarter-period current pulse (270 kV) is applied by a 1 Ω LC-water-line Marx generator. Typical upstream and downstream currents, measured by Rogowski coils, are shown in Fig. 2b. The plasma is produced using a cylindrical flashboard that is placed 6.5 cm outside the 85%-transparency anode, and driven by a 0.9 μ F, 24 kV capacitor. Two optical systems that image the same plasma section onto the input slits of two spectrometers are used for observation along the axis. The spatial resolution in the r and θ directions are 1 mm and 5 mm, respectively. The light from each spectrometer output slit is collected by a set of 10 photomultiplier-tubes (PMT's) to provide time-resolved measurements with a response time of 7 ns (FWHM)

The electron density (n_e) of the prefilled plasma, determined in-situ from hydrogen line Stark broadening and MgII (doping) line ratios, is $(2.2 \pm 0.5) \times 10^{14}$ cm^{-3} over the entire A-K gap. The electron temperature (T_e), also determined from MgII line ratios, is (5.5 ± 0.5) eV,

with a plasma injection velocity of $(3-10) \times 10^6$ cm/s. The plasma is composed mainly of protons, with the rest being CIII-CIV ions. Near the cathode, the carbon fraction ($Z_1 n_1 / n_0$) is only 10%, while closer to the anode, the carbon fraction is $\sim 30\%$.

Axial resolution is obtained by observing light emission from a narrow column of impurities injected into the plasma. A Nd:YAG laser pulse (10 ns FWHM, <100 mJ) is used to evaporate solids deposited on either of the POS electrodes creating an impurity plasma column with $\approx 45^\circ$ divergence angle that flows into the POS region (column width <1cm).

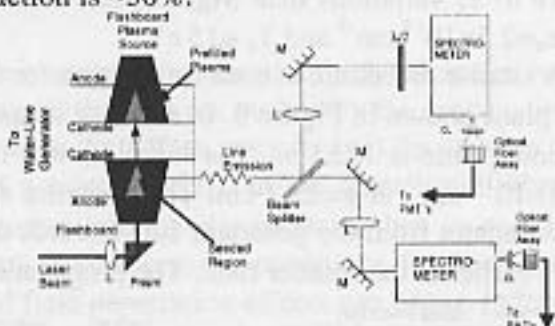


Figure 1 The POS and spectroscopic systems. M, L and $\lambda/2$ represent mirrors, lenses and half-wavelength plate, respectively

III. Experimental Results

The evolution of n_e and T_e during the POS operation is studied by observing the intensities of MgII, AlII, and AlIII lines that are emitted from levels of various excitation energies. The line intensities depend on the axial and radial positions and on the POS conduction time. In order to study the changes in the densities of the emitting ions, their axial velocities (v_z) were determined from Doppler shifts, and were seen to remain relatively low (e.g., the peak v_z of CIII is $<1 \times 10^7$ cm/s). During the pulse, the CIII moves axially <0.4 cm, which cannot affect n_e significantly. Measurement of the radial velocity was not performed in our experiment, but at all radii (at a given axial position) the temporal behavior of the intensity is similar to within 25 ns. For the ions to cross the A-K gap requires that they would acquire a radial velocity $\approx 1 \times 10^8$ cm/s; with the measured v_z of CIII this implies a divergence angle of $\leq 6^\circ$, which is very unlikely.

Figure 2a shows the time-dependent level populations of the MgII 3p level (4.4 eV), the AlII 4s 1S level (11.8 eV), and the AlIII 4p level (17.9 eV), observed at the $r=2.5$ cm, $z=0$ (defined as the POS axial center, where negative z is towards the generator) with similar POS operation (shown in Fig. 2b). The intensity of all three lines increases, but the increase is larger for the higher levels, and the lines start to drop simultaneously at $t=(46 \pm 3)$ ns.

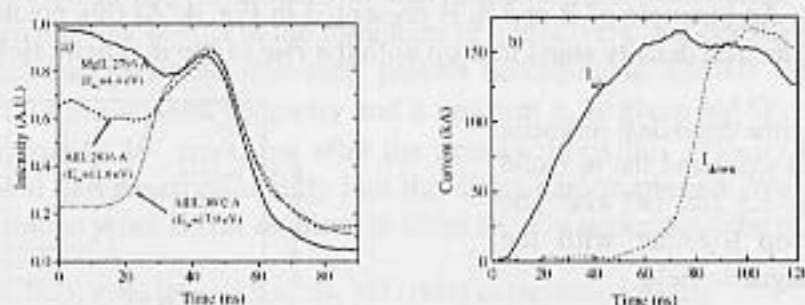


Figure 2. a) The time dependent intensity of an MgII line (solid), AlII line (dashed), and AlIII line (dotted) during the POS operation. b) The generator (I_{gen}) and load (I_{load}) currents.

Assuming that the density of the light-emitting ions does not change during the pulse, and by treating the three lines self consistently using detailed collisional-radiative calculations, we found that at $t=46$ ns, T_e increases to 12 eV while n_e decreases by 15%. Ionization can affect the ion density by only a few percent since the ionization times of AlIII,

AlIII, and MgII at these n_e and T_e are 4 μ s, 250 ns, and 180 ns, respectively. Furthermore, the intensity drop does not result from cooling of the electrons, since the AlIII is much more sensitive to T_e variations than MgII. A self-consistent treatment of the three lines at $t=70$ ns yields $n_e=2.5 \times 10^{13}$ cm $^{-3}$ and $T_e \cong 15$ eV.

A similar procedure at each r, z position for three different times yields the n_e contours in the $r-z$ plane shown in Figure 3. In all these shots, the POS conduction time is 65 ± 10 ns, and the opening time is 15 ± 3 ns. The initial n_e was taken to be 2.2×10^{14} cm $^{-3}$ at $-3.5 \leq z \leq 3.5$ cm, and 1.1×10^{14} cm $^{-3}$ at $z = \pm 5.2$ cm. The contours show that n_e increases before dropping. The drop propagates from the generator side towards the load, but the propagation is diagonal, i.e., n_e drops earlier at the smaller radii. The propagation velocity is $(1.5-2.5) \times 10^8$ cm/s.

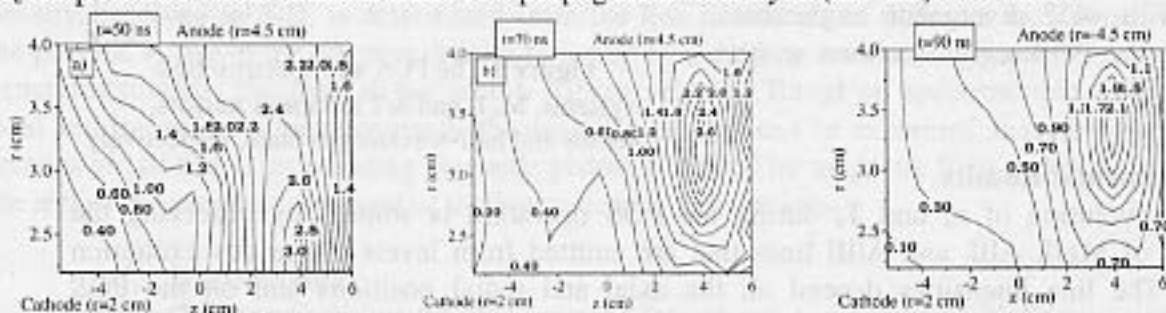
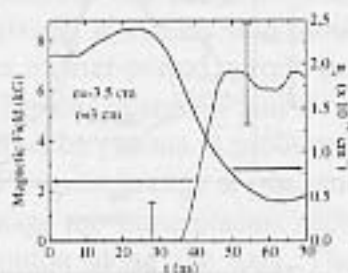


Figure 3. n_e contours in units of 10^{14} cm $^{-3}$, for a conduction time of 65 ± 10 ns, at a) $t=50$ ns; b) $t=70$ ns; c) $t=90$ ns. Negative z is towards the generator and the short-circuit load is at $z=+15$ cm.

At $t=50$ ns, n_e already dropped considerably at the generator-cathode side of the prefilled region but it increases at the load side, especially at the cathode side. At $t=70$ ns, when some current is already measured at the load, n_e decreases also at the load side of the plasma but only near the cathode. At $t=90$ ns, when the full current flows to the load, n_e drops everywhere to 10-30% of its initial value, except for a small region at the load-anode side.

The magnetic field (B) is measured from the Zeeman splitting of the 5609 Å line ($7p-7s$ transition) of PbII ions doped into the plasma. The spectral profiles of the π components (light polarized along B , in the θ direction) and the σ components (light polarized perpendicular to B , in the r direction) are observed simultaneously at each position with the two spectrometers. The two profiles are fitted self-consistently assuming a Doppler broadening and Zeeman splitting to obtain B . An example of B and n_e is presented in Fig. 4. At this position, as in all other positions, the electron density starts to drop with the rise of the magnetic field.

Figure 4. The time dependent magnetic field (dashed line, left axis) and the n_e (solid line, right axis) at $z=-3.5$ cm, $r=3$ cm. The density starts to drop together with the penetration of the magnetic field.



The velocities of carbon and doped ions of various masses and charges were studied from Doppler shifts, and the proton velocity was determined from time-of-flight measurements using an array of 4 magnetically-insulated Faraday cups inserted into the plasma (in a similar manner to that which was used to study the ion flow in the vacuum section between the plasma and the load [7]). Since the Faraday cups are saturated within a few ns, only the velocity of the fastest protons can be determined. The proton axial velocity is

observed to be $(3.5 \pm 1) \times 10^8$ cm/s. However, these measurements should be taken with a grain of salt since the velocity obtained may be the propagation velocity of the magnetic piston.

IV. Discussion

The models that describe the POS conduction account for the plasma dynamics in two different limits. In the limit of large plasma pushing all the ions are pushed by the propagating magnetic piston to the same velocity, which is between the Alfvén velocity (v_A) (in the case of specular reflection[8]) and $v_A/\sqrt{2}$ (in the case of a snowplow[2]). In the other limit, where EMHD[5] theory is valid, the magnetic field penetrates into the plasma faster than v_A and the ions are almost immobile. At our POS and plasma parameters, the conditions for neither of these limits are satisfied, and both ion pushing and field penetration effects can occur. Indeed, the density was shown to increase and then decrease, a behavior similar to that observed in longer conduction-time POS's where it was explained as MHD pushing followed by EMHD effects[2]. In our experiment, the velocities of the heavy ions are low and their motion is small. Only the protons may move significantly on this short time scale, a motion that results in a drop of the electron density by the factor determined by the fraction of protons in the plasma. This is consistent with the fact that the density does not drop to zero, and that the decrease at larger radii is smaller, since the proton fraction is smaller at larger radii.

The magnetic field measurements indicate that protons are pushed by the magnetic piston, since the density increases ahead of B, and at each position B penetrates into the plasma together with the drop in n_e . However, the mechanism for the different behavior of the protons and heavier ions is not clear yet. The dynamics of a multi-component plasma interacting with magnetic pressure were described by Mendel[9] in the context of plasma-filled ion diodes. The magnetic pressure developed in the magnetic piston propagating through the plasma pushes the electrons and the ions that have kinetic energy smaller than the Hall potential (in the piston frame-of-reference). Ions with larger energy, namely the heavier ions, can "climb" the potential hill and stay behind the piston. In the laboratory frame the reflected ions would acquire a high velocity ($\sim v_A$) while the heavy ions acquire a much lower velocity, depending on the time they spend inside the piston. However, in our experiment the density of the plasma composed of carbon ions and electrons is quite high, a few times 10^{13} cm⁻³, and the mechanism for such plasma-leakage across the piston is not understood as yet.

Another question is the mechanism of the magnetic field penetration into the dilute plasma. The proton pushing results in the formation of a relatively low-density carbon plasma. The magnetic field can penetrate into such plasma according to EMHD theory. The Hall penetration velocity for a coaxial geometry and a uniform n_e is given by[5]: $v_H = cB/(4\pi n_e r)$. For our initial n_e , $v_H = 7 \times 10^7$ cm/s, but after the density drops this velocity becomes much higher, and the field can penetrate rapidly into the dilute carbon plasma. We emphasize that considerable theoretical work is still required in order to fully understand the observations.

¹ B. V. Weber, et. al., IEEE Trans. Plasma Sci., **19**, 757 (1991) and references therein.

² B. V. Weber, et. al., Phys. Plasmas **2**, 3893 (1995) and references therein.

³ G. G. Spanjers, et. al., IEEE Int. Conf. on Plasma Sci., 160 (Madison, WI, USA, 1995).

⁴ R. Shpitalnik, et. al., Phys. Plasmas **5**, 792 (1998).

⁵ A. Fruchtman and K. Gomberoff, Phys. Fluids B **5**, 2371 (1993).

⁶ M. Sarfaty et. al., Phys. Plasmas **2**, 2122 (1995).

⁷ Ya. E. Krasik and A. Weingarten, IEEE Trans. Plasma Science **26**, 208 (1998).

⁸ M. N. Rosenbluth, in "Progress in Nuclear Energy, Series XI: Plasma Physics and Thermonuclear Fusion research", (Pergamon, London, 1963), Vol. 2, pp. 217-277.

⁹ C. W. Mendel, Jr., Phys. Rev. A **27**, 3258 (1983).